# WIND DATA ANALYSIS AND WAKE MODELING FOR A SINGLE WIND TURBINE ON FLAT TERRAIN

**Leandro J. L. Stival, leandro.stival@ufpr.br**
**Alexandre K. Guetter, guetter.dhs@ufpr.br**
Federal University of Parana and Post-graduate Program on Water Resources and Environmental Engineering, #210 Coronel Francisco Heraclito dos Santos Ave, Curitiba, 81531-990, Brazil

**Fernando O. Andrade, fandrade@utfpr.edu.br**
Federal University of Technology - Parana and Post-graduate Program on Water Resources and Environmental Engineering, #5000 Deputado Heitor Alencar Furtado St, Curitiba, 81280-340, Brazil

***Abstract.*** *The recent significant increase in wind power potential assessments and energy production is explained by the global availability of wind resource and technology advances with costs that has been falling. Wind energy efficiency depends on the atmospheric processes and turbulence effects at the wind turbine generator(WTG). It is essential to study the efficiency by assessing the effects that wind parameters and wakes will have on the whole system. Hence, a complete assessment of wind resources is crucial to retain full advantage of wind power. This study aims to investigate the efficiency of wind energy generation in two North American Wind Farms, through wind data analysis and wake modelling. The data analyzed are the SCADA data, met mast data and the collected by LiDAR measurements. The wind data analysis was performed trying to identify and determine parameters of importance for the power performance of the wind turbine. The goal of the wake models employed in energy yield prediction software is to represent the turbine induced wind speed deficits and the ratio of restoration to the freestream velocity. The simplified models consider the wake to be consistent and axisymmetric for increasing the solving velocity and are established on the conservation of mass and empirical association of wake decay, such as the model implemented at this work, the PARK model, which considers the radial velocity to be constant inside the wake and expanding radially at the rate of decay constant times downstream distance. The measurements from the LiDAR was compared with the PARK model, which was developed for a single turbine on a flat terrain. This PARK model seemed to over predict most part of the wake in comparison with LiDAR measurements.*

***Keywords****: wind power, wake modelling, LiDAR, wind analysis.*

## 1. INTRODUCTION

The demand for energy has been increasing in the last decade due to the global economic growth, thus wind power has gained respect in terms of progress and potential as a clean resource. This selective evolution is explained by the extreme availability of resource, a reason that has brought a growing success and has pushed the development of wind farms. Due to the fast growth in the number and size of installed wind farms around the world, it is essential to study the efficiency by assessing the influences of the wind parameters and wake characteristics over the whole system. Hence, a complete assessment of wind resources is crucial to retain full advantage of wind power.

Wind turbines generate wakes, which are areas of flow with lowered momentum and enlarged turbulence. Such phenomena is induced by the energy extraction from the wind, where each wind turbine produces a turbulent region with slower wind velocities downstream, thus leading to decreased energy yield for the downstream wind turbine. The development of the wake affects power output, because of that, it is essential to be able to quantify and predict the magnitude of uncertainties and the characteristics of the flow behind the turbine. It is imperative to have a valuable comprehension of the performance of wakes in wind power plants with the objective of diminishing power losses and increasing lifetime of the blades.

Turbine wakes are responsible for important power losses in wind farms (Bastankhah & Porté-Agel, 2014). For wake losses around 10 to 20% of power output in wide wind plants, precise measurements of wake length and width are crucial for wind farm preparation and optimization (Hansen and Barthelmie, 2009). Sanderse (2009) demonstrated that over different wind directions in a given wind farm the losses can represent 5 to 8% of the annual energy yield. Because of that, it is necessary for wind park developers to be able to predict quantitatively and with small uncertainties the extent and characteristics of the flow downstream of wind turbines (Tsalicoglou , 2012).

Although numerical and experimental techniques have become increasingly sophisticated and accurate in recent years, simple analytical models are still useful to predict wind-turbine wake flows and their effect on power production. The simplified models commonly used by the industry are scarce in the physical representation of the phenomena in comparison to most of the advanced methods based on computational fluid dynamics (CFD). However, an important advantage of these models is the lower computational cost when compared to the more complex models, which are not always able to represent the wakes accurately.

The simplified models establish linear momentum balance and they consider a consistent and axisymmetric wake. Most of them establish momentum conservation at the wake area, which expands in agreement with the wake development behavior (Réthoré, 2009). Some quick models represent the wake expansion straightly, such as the Jensen model (Jensen, 1983) employed in this paper.

## 2. MATERIALS AND METHODS

### 2.1 Study Area

The study area is located in the United States of America. Due to contractual agreement, it was not possible to describe the site location and its detailed information. In order to capture the freestream wake dispersion, the Galion was mounted in a specific wind turbine generator (WTG), which is located at the first row of WTGs in the southern portion of the wind plant. The measurement campaign consisted of six weeks with a long range Galion LiDAR that took place from September 14th, 2011 until October 26th, 2011. A mounted nacelle deployment was selected at the site due to the retractable back door on WTG, which enabled relatively easy installation and concurrent measurements through the horizontal plane of the wake. The WTG of interest had a Plane Position Indicator (PPI) scan trying to understand the single wake analysis behind it. The PPI scan mode consists in a constant elevation angle and fluctuate its azimuth angle, then the results could be projected on a horizontal plane. The scan was carried out with 81° width in ± 3° azimuth increments centered on the 180° axis straight out behind the WTG. It produced a 29-beam scan file that took nearly four minutes to finish a scan period (SgurrEnergy, 2011). Close to 300 m west of the WTG, a met mast was implemented, in order to have the concurrent wind measurement data, to regulate the wind direction calibration pertinent to the WTG yaw angle, and freestream wind speed. The wind direction region of importance was established for study as 90° until 270°, representing the south area, where winds from this region allow the evaluation of a single wake in the freestream.

### 2.2 Data Analysis

Once the measurements were recorded, data was screened to eliminate redundancy or insufficient period records. Due to the varied formats of the data sets, preliminary data evaluation and analysis were performed in order to converge the sources. The first step in any evaluation is performing a basic screening of the measured wind data. This basic screening was important to look for the following occurrences as: extreme wind speed values and sectors with extreme wind gradient exponents, which are typically seen when the data is of poor quality.

Acquiring a valid set of data of the wind direction during the period of production is very important due to the large variation in wind farm production over just a few degrees. Wind rose diagrams help to visualize the wind patterns at the site. When used clearly, it enables you to have greater knowledge to make better decisions, being the most common instrument to display wind data in terms of wind velocity and frequency distribution.

The influence of the wind speed parameters is important on wind turbine performance. Therefore, the statistical analysis of wind speed was performed with several sets of wind profiles, considering the diurnal variation of wind characteristics, frequency and histogram of wind speed. The turbulence intensity, obtained from straight measurements of horizontal turbulence fluctuations at the site, was also considered in the analysis. It was calculated by the ratio of the standard deviation of the wind speed ($s$) in (m/s), with a time step of each 10-minute period, divided by the corresponding mean wind speed ($V$), in (m/s), at the 80m height, as the following,

$$TI = \frac{s}{V}. \quad (1)$$

### 2.3 Wake Modelling

The PARK model developed by Jensen (1983) represents a gradually extending wake with a velocity deficit reliant on distance, that has a regular value across its width and height, as illustrated in Fig. 1. The model considers a top-hat shape for the velocity deficit in the wake, and a gradually developing wake with a velocity deficit that is only relative to the distance downstream from the rotor, meaning that the wake expands radially at the rate $k\,X$.

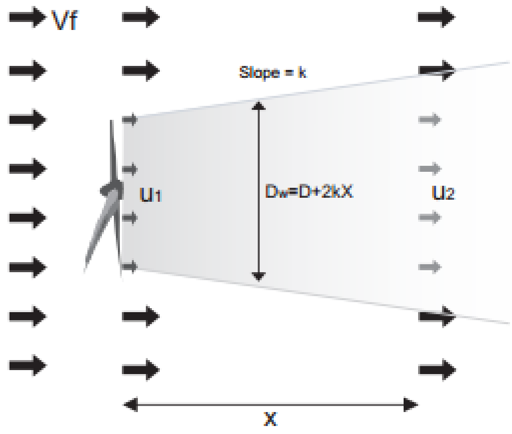


Figure 1. Schematic view of the PARK model wake expansion.

Firstly, the wake decay constant (*k*) was determined, which represents the dissipation of the wake as the wake width increases. A strong wake decay means a rapid decrease of the wake and large wake width. Previous work showed that the value of *k* is usually taken as 0.075 for onshore wind farms. Offshore wind farms use a value of 0.04 – 0.05 (Barthelmie et al., 2006; Barthelmie et al., 2009). In this work, the wake decay constant was calculated according to;

$$k = \frac{\alpha}{\ln(\frac{h}{z_0})}, \tag{2}$$

where α is the induction factor, which is a reduction of the wind velocity between the freestream to the rotor; *h* is the WTG hub height; *Zo* is the surface roughness.

The model width, *Dw*, was determined from the rotor diameter, *D*, the wake decay constant given by Eq. (2) and the longitudinal downstream distance, *X*, as the following,

$$D_w = D + 2kX. \tag{3}$$

Eq. (4) describes the PARK model wake profile (*PP*),

$$PP = 1 - [(1 - ((1 - C_t)^{\frac{1}{2}}))] \cdot [\frac{D}{D_w}]^2, \tag{4}$$

where the width is used together with the trust coefficient, *Ct*, and rotor diameter, *D*. The thrust coefficient values depend on the power curve and track down for each inflow wind speed.

The analysis of wake modelling involves comparisons with measured data, where a wake profile was computed for each 10-minute period in the filtered dataset. The standard error (SE) was applied to the plots using error bars, which was calculated as the ratio of the standard deviation (s) over the square root of the number of counts (n), as follows,

$$SE = \frac{s}{\sqrt{n}}. \tag{5}$$

The ten-minute average dataset in the LiDAR measurements were associated with the hourly resolution of the inflow met mast data. This enables the LiDAR data to be binned by inflow wind speed, so it was possible to represent the results as a percentage of the inflow. It was also possible that the inflow wind speed could be assessed at intervals of 1 m/s, and so determine the respective wake recovery obtained by the PARK model.

## 3. RESULTS AND DISCUSSION

The data presented at this section is crucial for the characterization of a wind farm profile. The data obtained by the meteorological mast was used as an input in the Windographer software, which produced results that comprehend the measurement campaign and analysis of wind characteristics.

The mean wind speed from the meteorological mast data was 5.09 m/s, where the operational wind speed range of the WTG is varied between 4 m/s to 25 m/s. Thus, the measurement campaign was implemented during a low wind speed period. The mean wind direction close to 183° at site was in agreement with the sector proposed in the methods section, where it was assumed to deploy in the sector range of 90° to 270°, representing the southern sector. The mean temperature around 15°C represents that the Galion LiDAR was inside of the viable range of the 40°C during the deployment period. The variables measured by the meteorological mast are presented in Tab. 1.

Table 1. Meteorological mast variables.

| Variable | Mean |
|---|---|
| wind speed (m/s) | 5.09 |
| wind speed standard deviation (m/s) | 0.64 |
| wind speed variance | 0.41 |
| maximum wind speed (m/s) | 24.1 |
| minimum wind speed (m/s) | 0 |
| turbulence intensity | 0.13 |
| wind direction (°) | 183.2 |
| temperature (°C) | 15.3 |
| pressure (kPa) | 839.4 |
| air density (kg/m$^3$) | 10.1 |

Assessing the energy that can be generated at a specific site is essential. It requires the estimation of the probability density function (PDF), which is indispensable for several wind power applications. The Weibull distribution is extensively applied to establish wind frequency distribution on wind power and other renewable energy sources. The frequency distribution of the meteorological mast and the two parameters Weibull distribution are presented in Fig. 2.

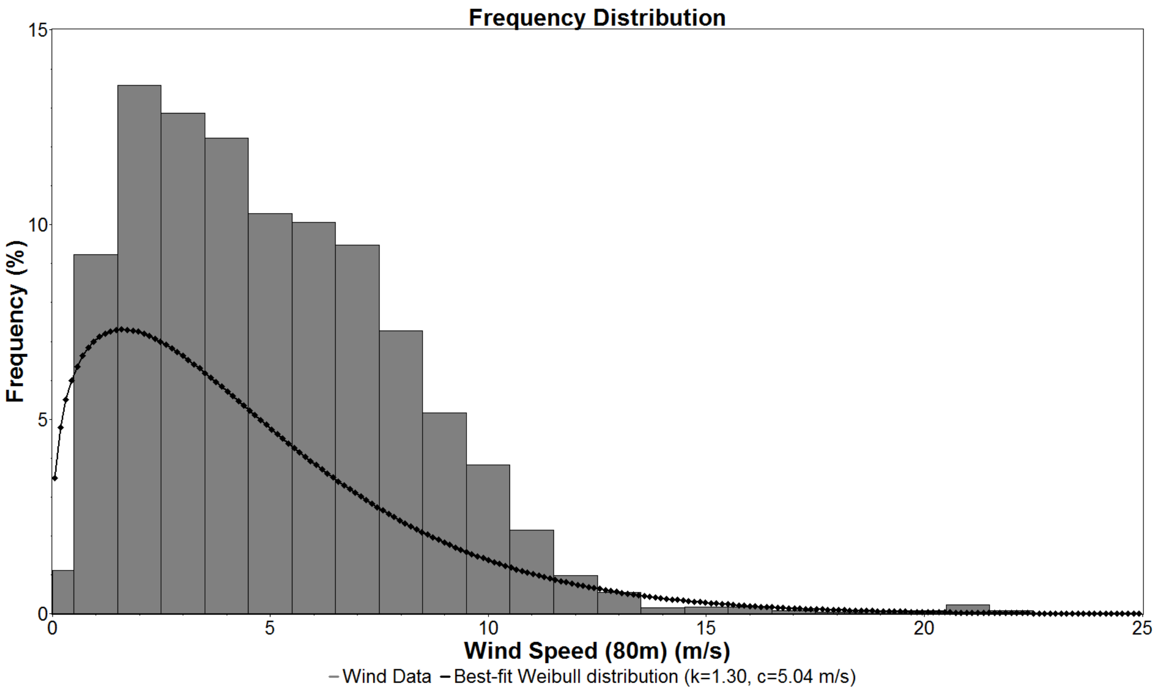


Figure 2. Met Mast Frequency Distribution.

The Weibull fit determined by the software is the maximum likelihood algorithm, where the crucial elements of the Weibull distribution are the behavior linked with the shape parameter, k, and the scale parameter, c, identifying how those parameters affect the distribution. The shape parameter, k, is equivalent to 1.30, which means that a lower number is related to a wide distribution, where the wind velocity is likely to vary considerably. The Weibull parameter, c = 5.04 m/s, can affect the distribution in terms of changes on the abscissa scale. Increasing c, the distribution extends to the right and its height declines, while decreasing c, the distribution contracts to the left and its height rises.

The wind rose found from met mast data is shown in Fig. 3. Winds from the southern sectors were prevalent, dominating around 65% of the occurrences, which represents the region of interest from 90° to 270°. However, when it was assumed that the cut in velocity was 4 m/s, the percentage increased to 70%.

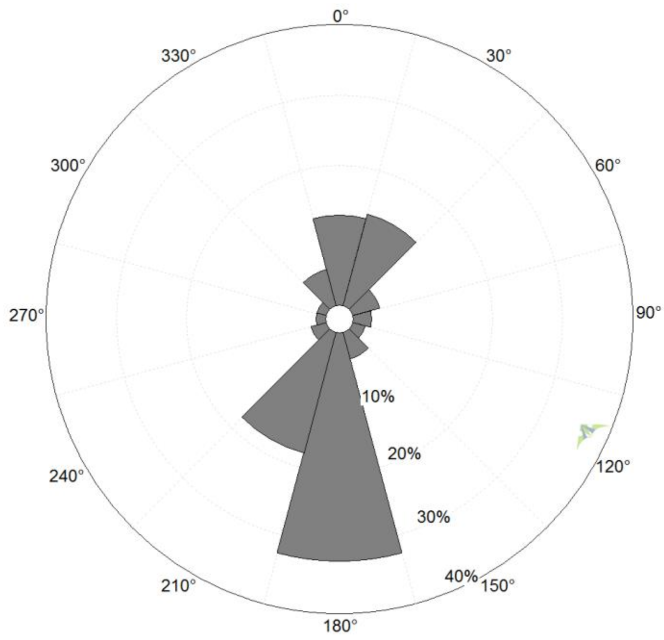


Figure 3. Wind Rose.

Once the statistics of the wind data from the meteorological mast were analyzed, with the objective of understanding the micrositing behavior, they were used as initial and boundary conditions to perform the wake modelling. The parameter used as the models input data (inflow conditions) was the freestream wind speed.

The inflow conditions were chosen for 1 m/s bins, where the range of interest varied from 5m/s to 12 m/s. In order to compare the Galion LiDAR measurements with the PARK model, the model parameters were defined and the wake decay constant was calculated by the Eq. 2, where $h$ was taken as 80 m, $Zo$ was 0.03m (WMO, 2008) and α was equal to 0.5 (SgurrEnergy, 2011), then resulting in $k = 0.063$. The downstream distance, $x$, was defined to be a ratio of the rotor diameter, $D$, for this reason the variable wake diameter, $Dw$, was also defined in terms of $D$. The thrust coefficient was related to the power curve and results in different values for each binned wind speed, but for contractual reasons it was not possible to present the coefficients.

With the objective of investigating the impact of wind speed on the model performance associated with LiDAR measurements, each velocity bin was plotted and shown in Fig.4 and 5 individually. The ordinate axis represents the normalized freestream recovery, which presents the velocity deficits behavior. The abscissa axis shows the downstream distance behind the wind turbine in terms of rotor diameters ($D$). There are two profiles represented in the graphs, the PARK wake model is shown as black triangles with a short dash line linking those and LiDAR measurements represented as white circles with error bars, where each bar corresponds to ± 1 standard error. The error bars seem to have an increasing pattern starting at 10 rotor diameters downstream, which is valid for a 5 m/s to 9 m/s wind speed bin. The 10 m/s bin presents a similar pattern, but there is a lack of data at 12 rotor diameter, which means that the bin presents only 11 points. Note that the next two bins, 11 m/s and 12 m/s, present downstream distances until 9 rotor diameters. This was mainly because of the poor data recovery on LiDAR measurements at those bins associated with the distance downstream of the WTG. Also, the two bins do not have a pattern in the error bars, the 11 m/s wind speed bin is the first bin which is shown in the highest values of the error bars at 1 and 2 rotor diameters, which means closer to the upstream WTG.

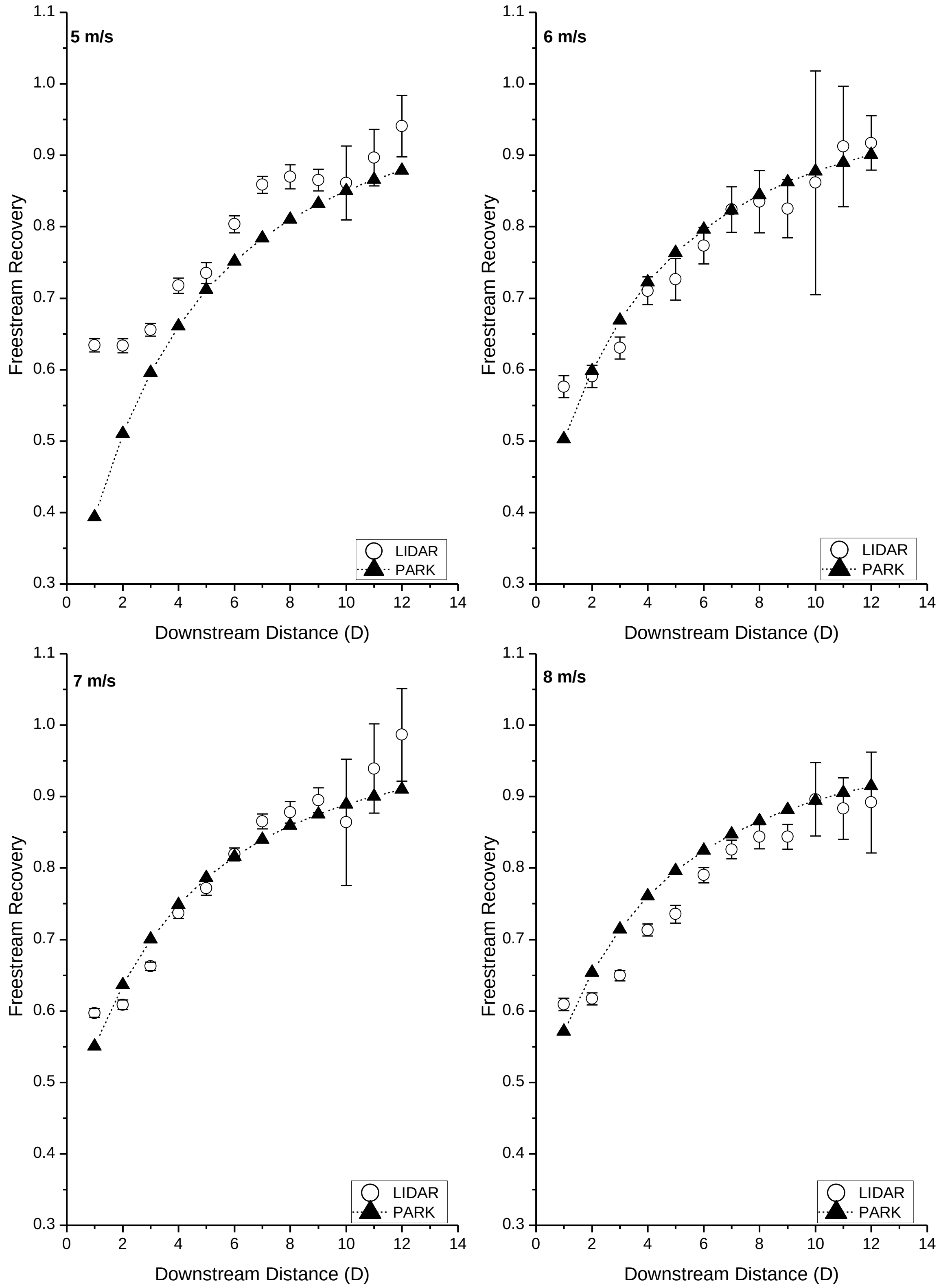


Figure 4. Freestream Recovery 5 to 8 m/s.

In the 5 m/s inflow conditions, bin shows 38% and 19% difference in 1 and 2 rotor diameters respectively, between the LiDAR measured wake and the one predicted by the PARK wake model. Outside this region the model shows more similarity to the measurements and the 11 and 12 rotor diameter downstream presents points where the PARK model is inside the range of the error bars. In general, the PARK wake model under predicts the recovery until about 9 rotor diameters and afterwards the LiDAR measured wake exhibits increase in the error bars associated to low data counts.

In the case of the 6 m/s inflow conditions, bin shows a slightly greater deficit than in the 5 m/s bin, where the highest difference was 13% at the first rotor diameter downstream. Following this region, the model had a great agreement to the LiDAR measurements, since most of the points of the model positioned inside the LiDAR error bars range. There was a slightly lower deficit in the LiDAR data profile with the two crossing each other twice, approximately 3 and 11 rotor diameters downstream. However, it is worth to mention that the increase in the error bars, being large at 10 rotor diameters, was due to the high standard deviation and lower data counts. The PARK wake model then slightly over predicted the recovery of the freestream speed.

For the cases of 7 and 8 m/s inflow conditions, bins are characterized for presenting lower standard errors due to the larger wind data counts. Both bins presented high agreement with all the points showing equal or less than 10% difference between LiDAR data and wake modelling profiles. However, the 7 m/s LiDAR data bin presented slightly higher freestream recovery than 8 m/s bin.

Despite the good agreement of data presented in the previous comparisons, the same does not occur in general for the next four bins, showed in Fig 5. For these cases, the 9 m/s velocity bin presented the best agreement, although only the last three points converge inside the error bar range, and showing four marks with more than 10% difference between the two profiles, being 2 to 5 rotor diameters downstream. Even so, the error bars still follow the pattern of the previous wind speed bin. While in the 10 m/s bin the pattern is still the same, but the LiDAR profile is valid up to 11 rotor diameters due to the lack of the data at 12 rotor diameters. At this wind speed, bins are only at the two points where the wake model is inside of the error bar range, at 1 and 10 rotor diameters downstream. Moreover, there were seven marks with greater values than 10% difference between LiDAR measurements and the PARK wake model, presenting the highest disparity at 11 rotor diameters downstream with 55%.

The 11m/s wind speed bin presented over prediction of the PARK wake model relative to LiDAR data, where there were no matches in both profiles. Besides that, the greater differences were presented at the first section that comprehends downstream distance 1 and 2 rotor diameters, with a maximum of 42%, which could be attributed to a relatively lower wind speed density during the measurements campaign, therefore not following the greater initial recovery from the PARK wake model. The over prediction of the model still persists for the 12 m/s bin, until the last section, which represents downstream rotor diameters 8 and 9, where the error bars enclosed the wake model and presented a difference of 6% and 7%, respectively.

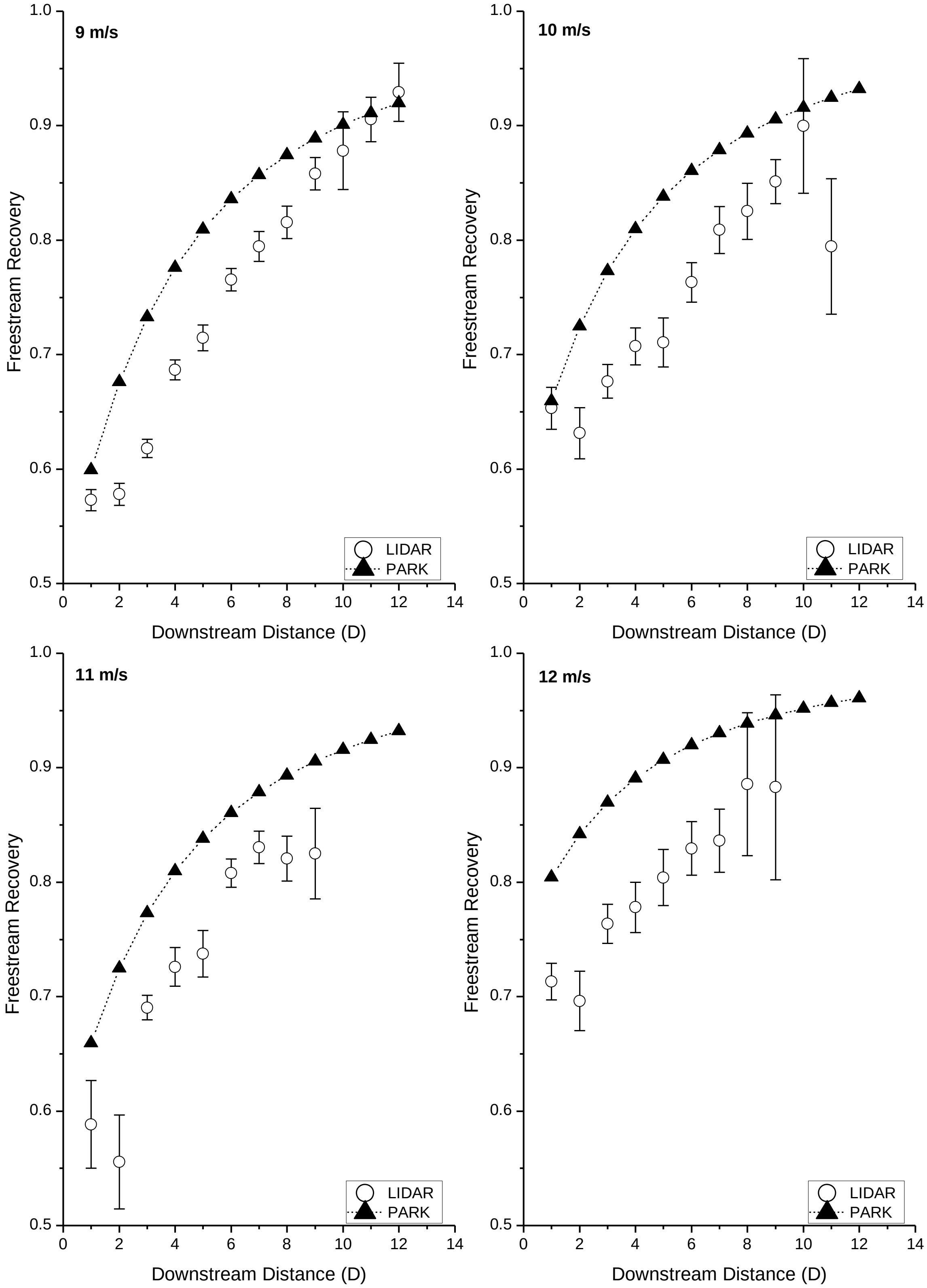


Figure 5. Freestream Recovery 9 to 12 m/s.

## 4. CONCLUSION

This study has examined the wake of a single WTG in the United States. The wind resource assessments were explored using the PPI scan of Galion LiDAR mounted on the WTG . The LiDAR measurement data was compared with the PARK wake model to evaluate the performance of the model in relation of LiDAR wake measurements for WTG. In order to investigate the WTG wakes, the wake decay length of the centreline was obtained from a PPI scan and binned an inflow condition of 1 m/s wind speed. Thus, the PARK wake model was then computed with a WTG and the normalized freestream wind speed for the campaign. After normalizing, the LiDAR wind data was compared to PARK wake model by binned inflow wind speed. Nonetheless, for distances greater than 9 rotor diameteres downstream, the quality of the LiDAR results showed a decay through the increase of the error bars associated to low data counts.

The PARK wake model was able to predict with good agreement the velocity deficit from the middle to the end section of the wake centerline, when taking into consideration the lower inflow wind speeds. This is consistent with the literature conditions of the PARK single wake model, which is designed to be valid in the far wakes. However, the model over predicted the downstream recovery, approaching the freestream inflow wind speed in comparison to LiDAR measurements at higher wind speeds. With better agreement in lower wind speed bins, they seemed to match each other for the most part of downstream distance. The two profiles have shown the best agreement with the lower inflow wind speeds and established a positive match for the 6 and 7 m/s wind speed bins.

## 5. ACKNOWLEDGEMENTS

This work was implemented with the support from SgurrEnergy, Vancouver office, Canada.

## 6. REFERENCES

Barthelmie, R.J., Folkerts, L., Larsen, G.C., 2006. “Comparison of wake model simulations with offshore wind turbine wake profiles measured by sodar ”. J. Atmos. Ocean. Technol., 23 (7), pp. 888–901.

Barthelmie, R. J., Hansen, K., Frandsen, S. T., Rathmann, O., Schepers, J. G., Schlez, W., Chaviaropoulos, P. K., 2009. “Modelling and measuring flow and wind turbine wakes in large wind farms offshore”. Wind Energy, 12(5), pp. 431–444.

Bastankhah, M., Porté-Agel, F., 2014. “A new analytical model for wind-turbine wakes”. Renewable Energy, 70, pp. 116-123.

Hansen, K. and Barthelmie, R. J., 2009. “Modelling and measuring flow and wind turbine wakes in large wind farms offshore”. Wind Energy, pp. 431-444.

Jensen, N. O., 1983. “A note on wind generator interaction”. Risø-M-2411, Risø National Laboratory Roskilde, pp. 1-16.

Réthoré, P-E. M., 2009. Wind Turbine Wake in Atmospheric Turbulence. Ph.D. thesis, Risø National Laboratory for Sustainable Energy, Roskilde, DNK.

Sanderse, B., 2009. “Aerodynamics of wind turbine wakes”. Technical Report, ECN-E- 09-016.

SgurrEnergy, 2011. “Investigation of Wakes using 2nd Generation Wind LiDAR”, message received by <gareth.brown@sgurrenergy.com> at 13 of January of 2016.

Tsalicoglou, C., 2012. Numerical Study of Wind Turbine Wake Aerodynamics in Uniform and Yawed Inflow. Msc. Thesis, Swiss Federal Institute of Technology, Zurich, CHE.

WMO, World Metereological Organization, 2008. Guide to Meteorological Instruments and Methods of Observation, No. 8 pp. I.5-12

## 7. RESPONSABILITY NOTICE

Leandro, Alexandre and Fernando are only responsible for the printed material included in this paper.